

# Synthesis and Radiopharmacology of *O*-(2-[<sup>18</sup>F]fluoroethyl)-L-Tyrosine for Tumor Imaging

Hans J. Wester, Michael Herz, Wolfgang Weber, Peter Heiss, Reingard Senekowitsch-Schmidtke, Markus Schwaiger and Gerhard Stöcklin

*Department of Nuclear Medicine, Klinikum Rechts der Isar, Technische Universität München, Munich, Germany*

The aim of the study was to develop a simple <sup>18</sup>F-labeled amino acid as a PET tracer for cerebral and peripheral tumors. *O*-(2-[<sup>18</sup>F]fluoroethyl)-L-tyrosine (L-[<sup>18</sup>F]FET) was synthesized and biologically evaluated. Results of the first human PET study are reported. **Methods:** No carrier added (n.c.a.) and D-[<sup>18</sup>F]FET were prepared by <sup>18</sup>F-fluoroethylation of L- and D-tyrosine in a two-step procedure. Biodistribution studies were performed in mice. The metabolic fate of L-[<sup>18</sup>F]FET was investigated in plasma, brain, tumor and pancreatic tissue samples using chromatographic procedures. Tumor uptake studies were performed in mammary carcinoma-bearing mice and in mice with the colon carcinoma SW 707. In a human PET study, a 59-y-old man with a recurrent astrocytoma was imaged using n.c.a. L-[<sup>18</sup>F]FET. **Results:** Synthesis of [<sup>18</sup>F]FET was accomplished in about 50 min with an overall radiochemical yield of 40%. The uptake of L-[<sup>18</sup>F]FET in the brain of mice reached a level >2% ID/g between 30 and 60 min postinjection. The brain uptake of the D-isomer was negligible, indicating blood-brain barrier penetration by a specific amino acid transport system. L-[<sup>18</sup>F]FET is not incorporated into proteins. High-performance liquid chromatography (HPLC) analysis of brain, pancreas and tumor homogenates as well as plasma samples of mice at 10, 40 or 60 min postinjection showed only unchanged L-[<sup>18</sup>F]FET. Activity uptake in the bone did not exceed 2% ID/g at 40 min postinjection. The brain uptake of L-[<sup>18</sup>F]FET in mice bearing mammary carcinomas and colon carcinomas reached 7.1% ± 1.2% ID/g and 6.4% ± 1.7% ID/g 1h postinjection, respectively. In the first human study, L-[<sup>18</sup>F]FET-PET allowed a clear delineation of a recurrent astrocytoma. Thirty-five minutes postinjection, the tumor-to-cortex ratio was >2.7. A tumor-to-blood ratio >1.5 was reached at 30 min postinjection and continued to increase. No significant activity accumulation was observed in peripheral organs after approximately 40 min postinjection. **Conclusion:** The high in vivo stability of L-[<sup>18</sup>F]FET, its fast brain and tumor uptake kinetics, its low accumulation in nontumor tissue and its ease of synthesis strongly support further evaluation of L-[<sup>18</sup>F]FET as an amino acid tracer for cerebral and peripheral tumors.

**Key Words:** PET; <sup>18</sup>F; amino acids; <sup>18</sup>F-fluoroethyltyrosine; FET; brain tumor

**J Nucl Med 1999; 40:205–212**

**P**ositron-labeled amino acids have clinical potential in oncology, neurology and psychiatry (1,2). For evaluation of brain tumors, amino acids are particularly interesting, as contrast is by far superior to that obtained with fluorodeoxyglucose (FDG) because of the low uptake of amino acids in normal brain tissue. Their use in clinical oncology is primarily based on the assumption of an increased accumulation of radiolabeled amino acids as biological building blocks necessary for tumor growth. In this model, an enhanced activity uptake in tumor tissue reflects an increased regional protein synthesis rate.

For this purpose, a variety of amino acids were synthesized and evaluated, as reviewed by Vaalburg et al. (2). An amino acid suitable for the evaluation of protein synthesis has to meet several criteria, such as high and fast incorporation rate and retention in proteins, insignificant metabolic pathways to nonproteins, rapid plasma clearance, high blood-brain barrier (BBB) permeability in the case of brain tumors and, last but not least, availability of a convenient labeling procedure. Some radiolabeled amino acids suitable for PET imaging fulfill these requirements: for example, L-[1-<sup>11</sup>C]leucine (3), L-[1-<sup>11</sup>C]tyrosine (4) and partly L-[methyl-<sup>11</sup>C]methionine (5) and L-[1-<sup>11</sup>C]methionine (6). Because of the short half-life of <sup>11</sup>C, great effort was also directed toward the synthesis and the evaluation of <sup>18</sup>F-labeled amino acids. Unfortunately, the two analogs, which exhibit protein incorporation, 4-[<sup>18</sup>F]fluoro-L-phenylalanine (7,8) and 2-[<sup>18</sup>F]fluoro-L-tyrosine (9–11), can only be synthesized with uncorrected yields <5%. More recently, a nucleophilic route for the production of <sup>18</sup>F-labeled aromatic amino acids was developed (1,12). However, the multistep synthesis introduces the fluorine in the first step and also leads to only low yields. Furthermore, the nucleophilic route is difficult to automate, and a robotic preparation must be used (12). Thus, synthetic problems result in a limited availability of these tracers, which prevent their widespread use.

During the revision of this article, synthesis and evaluation of another <sup>18</sup>F-labeled amino acid, L-[<sup>18</sup>F]fluoro- $\alpha$ -methyl tyrosine, was published (13). However, it is also

Received Dec. 2, 1997; revision accepted Apr. 28, 1998.

For correspondence or reprints contact: Hans J. Wester, PhD, Department of Nuclear Medicine, Klinikum rechts der Isar, Technische Universität München, Ismaningerstr. 22, D-81675 Munich, Germany.

prepared by electrophilic substitution, and the uncorrected yields are low and not sufficient for satellite distribution.

Because in vivo evaluation and kinetic modeling of the amino acid uptake in tumors indicated that transport is the dominating accumulation process and that irreversible trapping is of minor importance (1,14–16), artificial amino acids not incorporated into proteins are also useful tracers in oncology (17–23). A good example is the SPECT imaging of brain tumors (19,20,23) with [<sup>123</sup>I]-iodo- $\alpha$ -methyl-L-tyrosine ([<sup>123</sup>I]IMT) (21,22). Because IMT is not incorporated into proteins (20,23), imaging is based solely on changes of IMT transport kinetics.

The purpose of this study was to develop an easy-to-synthesize <sup>18</sup>F-labeled amino acid as a tracer for the imaging of brain and peripheral tumors based solely on amino acid transport. Derivation of the tyrosine hydroxyl group seemed to be the most straightforward approach. Tyrosine shows a high brain uptake (24), and the formation of an ether bond by fluoroalkylation should lead to a metabolically stable product. Because *O*-(2-[<sup>18</sup>F]fluoroethyl)tyrosine ([<sup>18</sup>F]FET) should not incorporate into proteins, no significant utilization in peripheral organs was expected.

## MATERIALS AND METHODS

### Chemicals and Radiopharmaceuticals

**Preparation of *N*-tert-Butyloxycarbonyl L-Tyrosine Methyl Ester.** *N*-tert-butyloxycarbonyl L-tyrosine methyl ester [*N*-BOC-(*O*-(2-fluoroethyl-L-Tyr))ome; 1g, 3.38 mmol] was dissolved in 2 mL of acetonitrile, and sodium methanolate (0.183 g, 3.38 mmol) was then added followed by 2-fluorotoloxoethane (25–27) (0.74 mg, 3.38 mmol). The solution was refluxed for 12 h. Purification was performed by reversed-phase chromatography (LiChrosorb RP-18, 250  $\times$  20 mm, 50/50 acetonitrile/water (vol/vol),  $k'$  = 3.3). The product fractions were combined, and the solvent was evaporated under reduced pressure to afford 622 mg (54%) *N*-BOC-(*O*-(2-fluoroethyl-L-Tyr))ome. Infrared (IR) (KBr)  $\nu$  = 3355  $\text{cm}^{-1}$ , 2975, 1772, 1681, 1520, 1448, 1366, 1245, 1225, 1167, 1074, 992, 923, 884, 836. <sup>1</sup>H nuclear magnetic resonance (NMR) (CDCl<sub>3</sub>, $\delta$ ) 6.75–7.12 (m, 4H), 4.67 (dt,  $J_d$  = 48 Hz,  $J_t$  = 4 Hz; 2H), 4.37 (t,  $J_t$  = 5 Hz; 1H), 4.17 (dt,  $J_d$  = 28 Hz,  $J_t$  = 4 Hz; 2H), 3.66 (s, 3H), 2.97 (d,  $J_d$  = 5 Hz; 2H), 1.37 (s; 9H). MS (EI)  $m/z$  (%) 341 ( $M^+$ , 0.7), 286 (77), 242 (91), 224 (79), 197 (48), 182 (37), 153 (100), 107 (52), 91 (3.5), 77 (3), 57 (15), 47 (3).

**Preparation of *O*-(2-fluoroethyl)-L-Tyrosine.** *N*-BOC-(*O*-(2-fluoroethyl-L-Tyr))ome (100 mg, 0.3 mmol) was treated with 2 mL trifluoroacetic acid (TFA) for 3 min (25). After the TFA was removed by a stream of nitrogen, 0.5 mL 0.1 mol/L sodium hydroxide was added to the residue and heated for 10 min at 80°C. Subsequently, the solution was acidified with 0.7 mL 0.1 mol/L hydrogen chloride and passed through a polystyrene cartridge (Merck, Darmstadt, Germany). After the cartridge was washed with 2 mL water, the product was eluted with 4 mL 50/50 ethanol/water (vol/vol). The solvent was removed under reduced pressure to afford 28 mg (41%) of the cold standard. IR (KBr)  $\nu$  = 3360  $\text{cm}^{-1}$ , 3135, 2975, 1596, 1506, 1396, 1249, 1036, 919. <sup>1</sup>H NMR (CDCl<sub>3</sub>, $\delta$ ) 6.78–7.25 (m, 4H), 4.75 (dt,  $J_d$  = 48 Hz,  $J_t$  = 4 Hz; 2H), 4.27 (dt,  $J_d$  = 28 Hz,  $J_t$  = 4 Hz; 2H), 3.37 (m, 1H), 2.82 (m, 2H). MS (EI)  $m/z$  (%) 228 ( $M+1$ , 1.5), 227 (6), 210 (1), 197 (9), 182

(27), 154 (68), 153 (100), 134 (13), 107 (98), 91 (21), 77 (34), 74 (8), 47 (12).

**Preparation of [<sup>18</sup>F]FET.** [<sup>18</sup>F]Fluoride was produced (25) by the <sup>18</sup>O(p,n)<sup>18</sup>F nuclear reaction by bombardment of an 98% <sup>18</sup>O-enriched water target with a 11 MeV proton beam at the RDS 112 cyclotron.

The aqueous [<sup>18</sup>F]fluoride solution was added to a 2.5-mL conical vial containing 0.25 mL dry acetonitrile (Merck, < 0.003% H<sub>2</sub>O), 5 mg (13.3  $\mu$ mol) Kryptofix 2.2.2 (Merck) and 5  $\mu$ L 1 mol/L potassium carbonate (Merck, suprapure). The solvent was evaporated under a stream of nitrogen at 90°C. Azeotropic drying was repeated at least twice (depending on the amount of target water) with 250- $\mu$ L portions of acetonitrile. [<sup>18</sup>F]FET was prepared by a two-step reaction that consisted of <sup>18</sup>F-fluorination of ethylene glycol-1,2-ditosylate (25,26) and subsequent <sup>18</sup>F-fluoroethylation of unprotected L-tyrosine (Fig. 1). Briefly, 4–5 mg (10–12  $\mu$ mol) ethylene glycol-1,2-ditosylate in 300  $\mu$ L acetonitrile was added to the dried kryptate [ $K^+ \subset 2.2.2$ ]<sup>18</sup>F<sup>-</sup> and heated at 90°C for 10 min. For the isolation of the <sup>18</sup>F-fluoroethyltosylate, the solution was purified by reversed phase high-performance liquid chromatography (RP-HPLC) (LiChrosorb RP-select B, 125  $\times$  8 mm, 50/50 CH<sub>3</sub>CN/H<sub>2</sub>O (vol/vol), 4 mL/min,  $k'$  = 5.7, preparative radiochemical yield 65  $\pm$  5%). After on-line fixation of the product fraction on a polystyrene cartridge (LiChrolut EN, Merck) and drying of the cartridge with nitrogen, the product was eluted with 0.9 mL dimethylsulfoxide (DMSO) into a second vial containing 4 mg of the di-potassium sodium salt of L-tyrosine (or D-tyrosine). The vial was closed and heated at 90°C for 10 min. After HPLC purification of the reaction mixture (LiChrosorb RP-18, 250  $\times$  8 mm, 10/87.5/2.5 ethanol/water/acetic acid [vol/vol/vol], 2.5 g/L ammonium acetate, pH 3.0, 4 mL/min,  $k'$  = 1.5), the collected fraction was passed through a strong cation exchange cartridge (LiChrolut SCX). After the cartridge was washed with 1 mL water, [<sup>18</sup>F]FET was eluted from the resin with 4 mL 0.15 mol/L phosphate-buffered saline (PBS; pH 7.4). Dilution with 2 mL isotonic saline solution and sterile filtration (Millex-GV 0.25 micron filter) into a sterile vial containing 1 mL 1 mol/L sodium bicarbonate led to the final formulation. For animal studies, a further dilution to approximately 1/20 of the original activity concentration was necessary.

Quality control was performed by HPLC (LiChrolut RP-18, 250  $\times$  4 mm, 10/87.5/2.5 ethanol/water/acetic acid [vol/vol/vol], 2.5 g/L ammonium acetate, pH 3.0, 0.5 mL/min,  $k'$  = 1.5), and thin-layer chromatography (SiO<sub>2</sub>; 95/5 acetonitrile/water [vol/vol],  $R_f$  = 0.06, lipophilic contaminant [ $\sim$ 2%–3%] at  $R_f$  = 0.62).

### Animals and Tumors

The experimental procedures used were approved and were in accordance with the guidelines on the use of living animals in scientific investigations. Biodistribution studies and tumor uptake were investigated in mice with xenotransplanted colon carcinomas

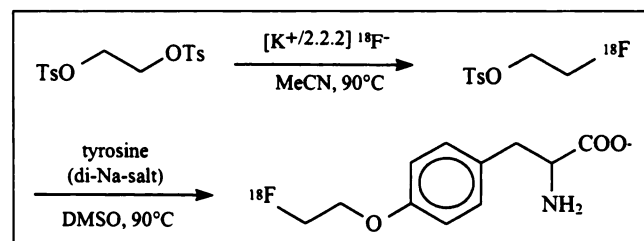


**FIGURE 1.** Synthesis of [<sup>18</sup>F]FET by direct <sup>18</sup>F alkylation of tyrosine.

SW 707 and mammary carcinomas (MaCaF). Experiments were performed 14–21 d after inoculation of the tumor cells. At this time, the tumors weighed 80–300 mg. Before the application of the radiotracer, the animals were anesthetized by diethyl ether. Subsequently, approximately 0.37–0.72 MBq (10–20  $\mu$ Ci) no-carrier-added (n.c.a.)  $^{18}\text{F}$ -FET in 100–200  $\mu\text{L}$  of PBS buffer was injected into the tail vein. The animals were killed by cervical dislocation at various times after injection, and the organs of interest were rapidly dissected. The radioactivity was measured in weighed tissue samples using a gamma counter. Data are expressed in mean  $\pm$  SD percent injected dose/g tissue ( $n = 3$ , unless otherwise stated).

## Pharmacological Studies

**Metabolic Stability of L-[ $^{18}\text{F}$ ]FET.** The extent of in vivo degradation of  $^{18}\text{F}$ -FET was analyzed by reversed-phase chromatography at 1, 10, 15, 40 and 60 min postinjection on plasma samples, 10, 40 and 60 min postinjection in brain homogenates, as well as at 60 and 180 min postinjection in tumor and pancreatic tissue. Blood samples were immediately centrifuged at 4000g. Speciation of the  $^{18}\text{F}$ -activity was performed using the supernatant solution after spiking with a small amount of cold  $^{18}\text{F}$ -FET by HPLC (LiChrosorb RP-select B, 125  $\times$  8 mm, 50/50  $\text{CH}_3\text{CN}/\text{H}_2\text{O}$  (vol/vol), 4 mL/min,  $k' = 5.7$ ). For studies on cerebral metabolism, brain tissue homogenates were prepared immediately after dissection. Nitrogen-frozen tissue samples were mechanically homogenized. The residue was taken up in 2 mL isotonic saline and centrifuged for 5 min at 6000g. The supernatant was separated from the pellet and both fractions were counted for  $^{18}\text{F}$  activity. The supernatant was then subjected to HPLC under conditions previously described for blood samples.

**Incorporation of L-[ $^{18}\text{F}$ ]FET into Proteins.** To determine the extent of protein incorporation of L-[ $^{18}\text{F}$ ]-FET, protein-bound activity in brain, pancreas, tumor and blood samples was determined at various points postinjection.

For this purpose, blood samples were immediately centrifuged at 4000g, and 250  $\mu\text{L}$  50% trichloroacetic acid was added to 750  $\mu\text{L}$  plasma and vortexed for 1 min. After centrifugation, the supernatant was removed from the pellet, and the  $^{18}\text{F}$ -activity in both fractions was determined using a gamma counter. Additionally, plasma samples were subjected to size exclusion chromatography. A BioSil SEC 125 column (300  $\times$  7.8 mm; BioRad, Richmond, VA) was used with 50 mmol/L sodium phosphate, pH 7.4, containing 0.1 mol/L NaCl as eluant at a flow rate of 1 mL/min. The elution profile was detected with an ultraviolet (UV) monitor at 254 nm. The radioactivity was measured in 0.5-mL fractions with a gamma counter. Incorporation of  $^{18}\text{F}$ -FET into tumor, pancreatic and cerebral tissue was measured as described previously.

**Brain Uptake of L- and D-[ $^{18}\text{F}$ ]FET.** To show specific uptake of L-[ $^{18}\text{F}$ ]FET in the brain by an amino acid transport system and to exclude other major uptake mechanisms, experiments also were performed with the D-enantiomer of [ $^{18}\text{F}$ ]FET in mice. The animals were killed at 10, 60 and 120 min postinjection. Brain uptake of the tracer was determined as described previously.

**Measurement of Partition Coefficient.** The partition coefficient of  $^{18}\text{F}$ -FET was measured using 2.0 mL octanol as the organic phase and 2.0 mL 0.1 mol/L phosphate buffer (pH 7.0) as the aqueous phase. Ten microliters of the radioactive sample in PBS buffer were added and mixed twice for 1 min at room temperature. The radioactivity of 200  $\mu\text{L}$  of each phase was measured after centrifugation.

## Patient Study

**Data Acquisition.** A 59-y-old man with a recurrent astrocytoma was studied using an ECAT EXACT 951/R scanner (CTI/Siemens, Knoxville, TN).

Details of the study were explained to the patient by a physician, and written informed consent was obtained. The axial resolution of the scanner at FWHM (full width half maximum) is approximately 5 mm; the transaxial resolution, 8 mm at FWHM. A dynamic emission sequence (8  $\times$  5 min) was started after intravenous injection of 296 MBq  $^{18}\text{F}$ -FET. After the dynamic emission scan of the brain, a whole-body scan spanning from the base of the skull to the bladder was performed (four overlapping bed positions, 5-min emission time per position, no attenuation correction).

Data were reconstructed by filtered backprojection using a Hanning filter with a cutoff frequency of 0.8 Nyquist. Attenuation was corrected with the standard separate ellipse algorithm provided by the scanner software. The image pixel counts were calibrated to activity concentrations (Bq/g), and standardized uptake values (SUVs) were calculated using the formula: SUV = tissue concentration/injected dose/body weight.

**Data Analysis.** To define regions of interest (ROIs), the frames of the dynamic study were summed between 30 and 40 min.

Tumor borders were defined by 75% isocontours in consecutive slices. An irregular reference ROI was placed in the contralateral cortex. To define the input function, small circular ROIs were placed in eight consecutive slices in the area of the right carotid artery, which was identified in the first frame of the dynamic study. Time-activity curves (TACs) were calculated for tumor, normal brain and blood. Using these TACs, the influx of L-[ $^{18}\text{F}$ ]FET in the tumor and normal brain was determined by Gjedde-Patlak analysis. Because the animal studies have shown that the blood activity only consists of unchanged [ $^{18}\text{F}$ ]FET, we have not performed plasma analysis in this first patient study.

## RESULTS

### Radiosynthesis

Depending on the concentration of tyrosine, the  $^{18}\text{F}$ -fluoroethylation led to saturation yields of up to 75%  $\pm$  5% after 6–7 min. These results were observed using a 45 mmol/L solution of the di-sodium salt of tyrosine in 300  $\mu\text{L}$  dimethyl sulfoxide. Decreasing the concentration to approximately 20 mmol/L led to a saturation yield of approximately 60% at reaction times of approximately 10 min. To facilitate HPLC-purification at the preparative scale, 25 mmol/L concentration was used. Starting with 3.6–9 GBq n.c.a.  $^{18}\text{F}$ -fluoride, the synthesis typically yielded 0.75–1.85 GBq  $^{18}\text{F}$ -FET in approximately 60 min with overall radiochemical yields of 40%  $\pm$  5% (based on  $^{18}\text{F}$ -fluoride), and a radiochemical purity between 97% and 99%.

### Biodistribution and Uptake Kinetics

Table 1 summarizes the tissue distribution data of  $^{18}\text{F}$ -FET in mice bearing SW 707 colon carcinomas. The uptake of  $^{18}\text{F}$ -activity in the bones did not exceed 2% ID/g at 40 min postinjection. The activity in the blood decreased from 4.30%  $\pm$  0.80% ID/g at 2 min postinjection to 1.40%  $\pm$  0.12% ID/g at 180 min postinjection. Except for the pancreas, in which approximately 18% ID/g was found at 60 min postinjection, no elevated organ uptake of FET was

**TABLE 1**  
Tissue Distribution of Radioactivity After Intravenous Injection of O-(2-[<sup>18</sup>F]Fluoroethyl)-L-Tyrosine (L-[<sup>18</sup>F]FET) into Colon Carcinoma-Bearing Mice

	Uptake (%ID/g)				
	10 min n = 9	30 min n = 6	60 min n = 9	120 min n = 3	180 min n = 3
Brain	1.49 ± 0.30	2.09 ± 0.39	2.17 ± 0.64	1.72 ± 0.24	1.03 ± 0.13
Colon	3.25 ± 0.58	3.44 ± 1.06	2.66 ± 0.72	1.69 ± 0.28	1.20 ± 0.14
Liver	3.35 ± 0.49	2.84 ± 0.40	2.52 ± 0.44	1.71 ± 0.08	1.16 ± 0.09
Blood	4.30 ± 0.80	3.36 ± 0.25	3.03 ± 0.59	2.10 ± 0.14	1.40 ± 0.12
Kidney	4.19 ± 0.72	3.57 ± 0.44	3.12 ± 0.54	1.96 ± 0.10	1.56 ± 0.12
Heart	3.67 ± 0.51	2.95 ± 0.32	2.62 ± 0.43	1.77 ± 0.07	1.29 ± 0.11
Pancreas	27.97 ± 4.42	17.90 ± 1.89	18.24 ± 5.89	16.93 ± 3.83	8.30 ± 0.74
Lung	3.47 ± 0.51	2.98 ± 0.36	2.44 ± 0.39	1.69 ± 0.08	1.18 ± 0.13
Spleen	4.20 ± 0.49	3.25 ± 0.62	3.08 ± 0.71	2.08 ± 0.26	1.35 ± 0.14
Muscle	3.32 ± 0.43	2.81 ± 0.43	2.40 ± 0.44	1.62 ± 0.06	1.17 ± 0.10
Skin	5.10 ± 0.78	4.96 ± 1.31	3.83 ± 1.40	2.08 ± 0.51	1.52 ± 0.61
Tumor	3.84 ± 0.92	5.64 ± 1.33	6.37 ± 1.67	3.13 ± 1.85	3.45 ± 0.29
Bone	1.69 ± 0.11*	1.96 ± 0.33†	1.74 ± 0.36‡	2.19 ± 0.49§	1.91 ± 0.27

\*2 min postinjection, n = 3.

†5 min postinjection, n = 3.

‡10 min postinjection, n = 3.

§20 min postinjection, n = 3.

||40 min postinjection, n = 3.

found in other organs sampled. Furthermore, the activity concentration in the liver and kidney did not exceed the activity concentration in the blood over the whole time of observation. The tracer uptake into the brain was fast and increased continuously up to 60 min postinjection (>2% between 30 and 60 min).

In Figure 2, the uptake kinetics of L-[<sup>18</sup>F]FET in the liver, kidney and blood are shown. These organs show a fast distribution of the tracer, completed in less than 5 min postinjection (Table 1) followed by a continuous renal clearance ( $t_{1/2}$  approximately 110 min) without renal reup-

take of the tracer. These kinetics are typical for all tissues, except for the brain and the tumor, which showed retention of the tracer (Fig. 3). Thus, the uptake of L-[<sup>18</sup>F]FET in the tumor of colon carcinoma-bearing nude mice reached a value of approximately 4% ID/g at 10 min postinjection and increased to  $6.37 \pm 1.67\%$  ID/g at 60 min postinjection (Fig. 3). After 1 h, the activity cleared from the tumor with a rate comparable to that of the other organs.

The tracer accumulation in mammary carcinomas (Ma-CaF) of nude mice at 60 min postinjection (not shown) was

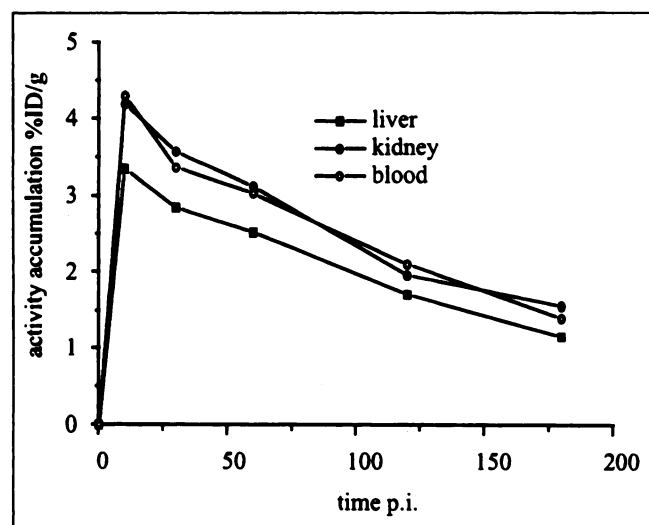


**FIGURE 2.** Uptake kinetics of L-[<sup>18</sup>F]FET in liver, kidney and blood of colon carcinoma-bearing mice.

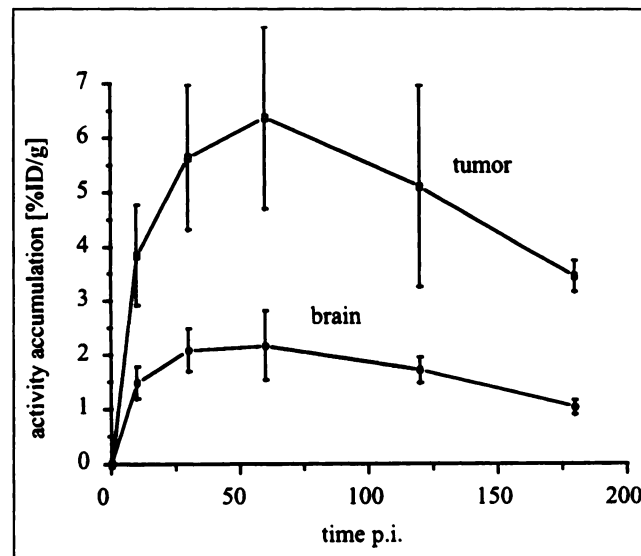


**FIGURE 3.** Uptake kinetics of L-[<sup>18</sup>F]FET in brain and SW 707 colon carcinomas of nude mice.

7.1 ± 1.1%ID/g (n = 3) and thus was comparable to that in colon carcinoma.

### Pharmacological Studies

The lipophilicity of FET was determined to be  $\lg P = -1.51$ , a value slightly lower than that of methionine (-1.07). TCA precipitation and size exclusion chromatography of plasma samples and pancreas, brain and tumor tissue at 60 min postinjection showed that the activity was not precipitable and was completely eluted in the low-molecular-weight fraction. No coelution with proteins was observed. At each time investigated, all of the activity extracted from tissue homogenates, spiked with cold FET, and analyzed on RP-HPLC, was coeluted with the cold standard.

To show specific brain uptake of L-[<sup>18</sup>F]FET by a stereoselective transport system, the brain uptake kinetics of D-[<sup>18</sup>F]FET in mice were also investigated. The curves in Figure 4 clearly show a lower BBB permeability for the D-isomer compared with L-[<sup>18</sup>F]FET. Whereas the uptake of the L-isomer reached a value of 2.43% ± 0.20% ID/g at 40 min postinjection, only 0.10% ± 0.01% ID/g were found for the D-isomer at 60 min postinjection.

### Patient Study

The dynamic PET study showed a rapid and intensive uptake of L-[<sup>18</sup>F]FET by the tumor tissue. At 10 min postinjection, the tumor could be clearly delineated from normal brain tissue (Fig. 5). The concentration (given as SUV) of L-[<sup>18</sup>F]FET, in both the tumor and normal cortex, continuously increased and reached 2.0 and 0.75, respectively, at 40 min postinjection (Fig. 5). Because of the slower accumulation kinetics in normal cortex, the tumor-to-cortex ratio continued to rise until the end of the study and reached a value of 2.7 at 40 min postinjection (Fig. 6). The blood curve showed a biexponential pattern with a terminal

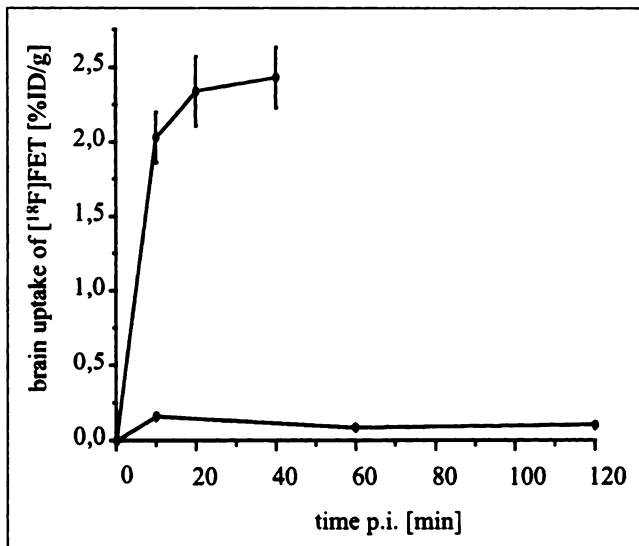


**FIGURE 4.** Stereospecificity of BBB transport of [<sup>18</sup>F]FET: time course of brain uptake of D-[<sup>18</sup>F]FET (lower curve) and L-[<sup>18</sup>F]FET (upper curve) in nude mice (n = 3).

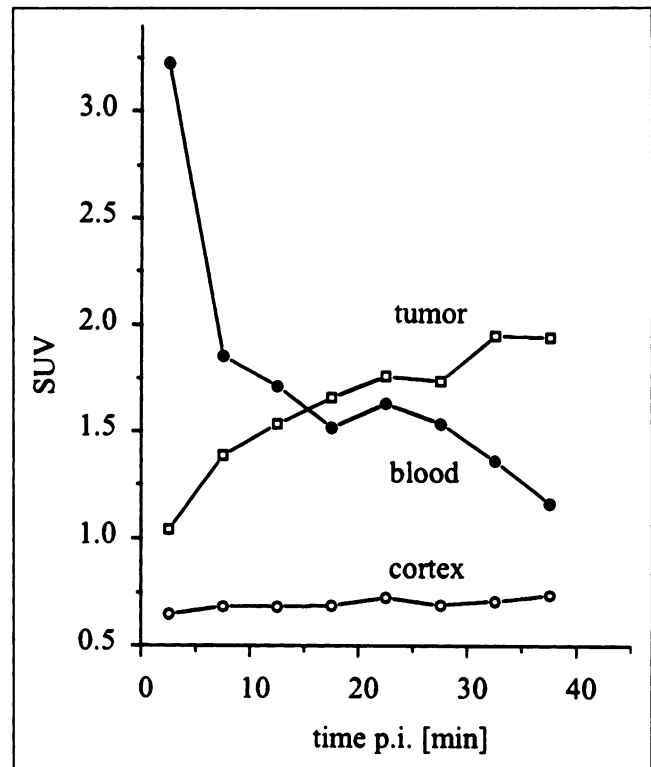


**FIGURE 5.** Time course of activity located in the blood pool (●), tumor (□) and reference tissue (cortex, ○) after intravenous administration of L-[<sup>18</sup>F]FET in patient with recurrent astrocytoma.

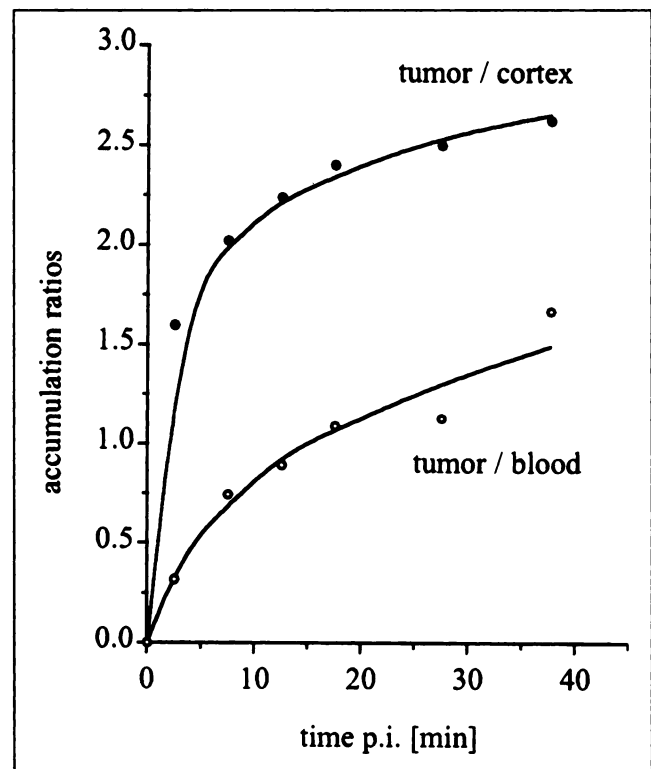


**FIGURE 6.** Time course of tumor-to-blood and tumor-to-cortex accumulation ratios of L-[<sup>18</sup>F]FET after intravenous administration of L-[<sup>18</sup>F]FET in patient with recurrent astrocytoma.

half-life of 40 min (Fig. 5). This led to a steadily increasing tumor-to-blood ratio until the end of the study period (Fig. 6).

The whole-body scan begun at 40 min postinjection showed tracer clearance by the kidneys. Remarkably, neither the liver nor the pancreas showed a higher L-[<sup>18</sup>F]FET uptake than the blood-pool activity (Fig. 7). No accumulation of the tracer in bone, bone marrow or intestine was observed.

## DISCUSSION

Because protein synthesis rate in normal brain tissue is several orders of magnitude lower than its glucose utilization (approximately 0.5 nmol/g/min for leucine versus 0.3 μmol/100 g/min for glucose [28]), amino acid tracers have been proposed as an alternative to FDG in the metabolic characterization of brain tumors (29). The clinical application of amino acid tracers has been severely limited by the lack of a tracer that is as widely available as FDG. Despite its complicated metabolism, [<sup>11</sup>C]methionine is the most frequently used agent. However, the short half-life of <sup>11</sup>C restricts its use to PET centers with an on-site cyclotron.

2-[<sup>18</sup>F]fluorotyrosine and *p*-[<sup>18</sup>F]fluorophenylalanine did not find routine application because of their difficult and low yield syntheses (10–12). The synthesis of L-[<sup>18</sup>F]FET, how-

ever, is simple and efficient and requires only commercially available chemicals and no sophisticated equipment. The <sup>18</sup>F-fluoroalkylation procedure is often used and is simple, starting from nucleophilic <sup>18</sup>F-fluoride (26,27). The entire synthesis is completed in less than 1 h, with a radiochemical yield of approximately 40% based on <sup>18</sup>F-fluoride.

The biodistribution of L-[<sup>18</sup>F]FET after intravenous injection of the tracer in mice was found to be as expected for an unnatural amino acid. Thus, no elevated activity accumulation was found in liver, kidney, heart or intestine. Blood clearance was somewhat slow. Interestingly, at each time investigated, the tissue-to-blood ratios are approximately 1 for all organs investigated, which is a good prerequisite for a clear delineation of peripheral tumors. Compared with all other amino acids studied thus far, L-[<sup>18</sup>F]FET shows the highest brain uptake at later observation times. Different from other unnatural amino acids such as IMT, which is not retained in the brain, but exhibits an early uptake maximum and is rapidly eliminated (20), the kinetics of L-[<sup>18</sup>F]FET in the brain indicated a longer retention by an unknown mechanism (30,31). A slow washout was observed only after 1 h. Because speciation studies on brain homogenates showed only the presence of the intact tracer, further experiments are needed to explain the retention.

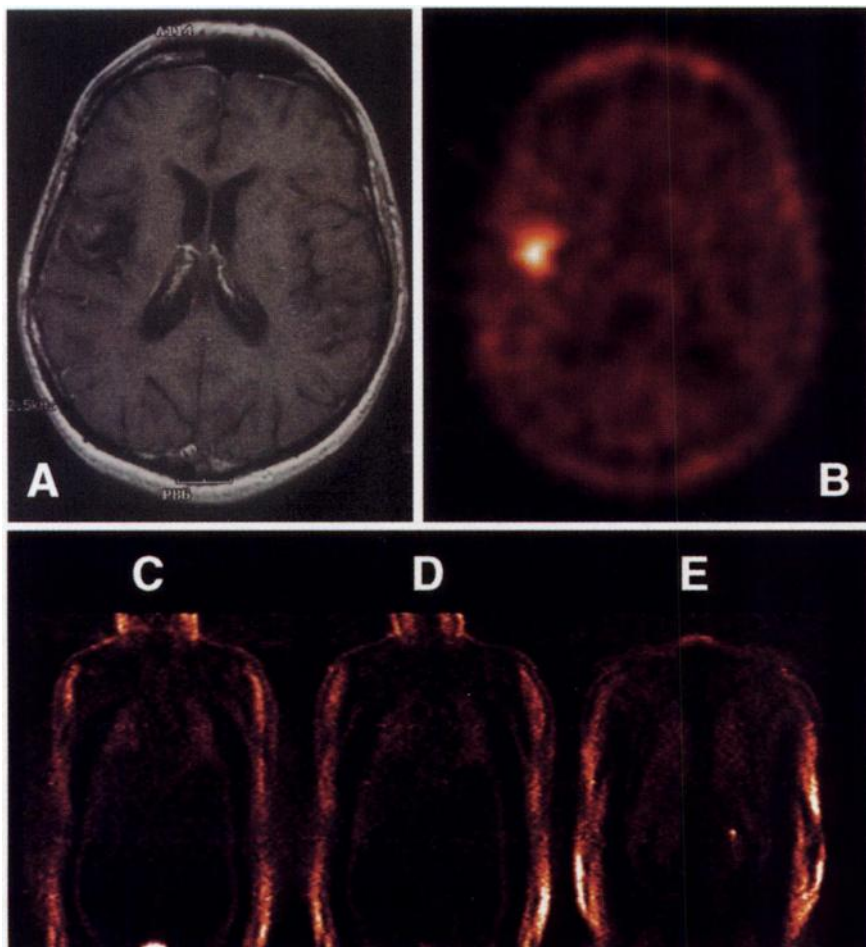


**FIGURE 7.** Comparison L-[<sup>18</sup>F]FET accumulation image (B) and T<sub>1</sub> weighted MR image after administration of Gd-DTPA (A) of patient with recurrent astrocytoma. Activity image was summed between 30 and 45 min postinjection of 296 MBq L-[<sup>18</sup>F]FET. Tumor borders were defined by 75% isocontours. Lower row: Regional body images of same patient (ventral to dorsal: C, D, E).

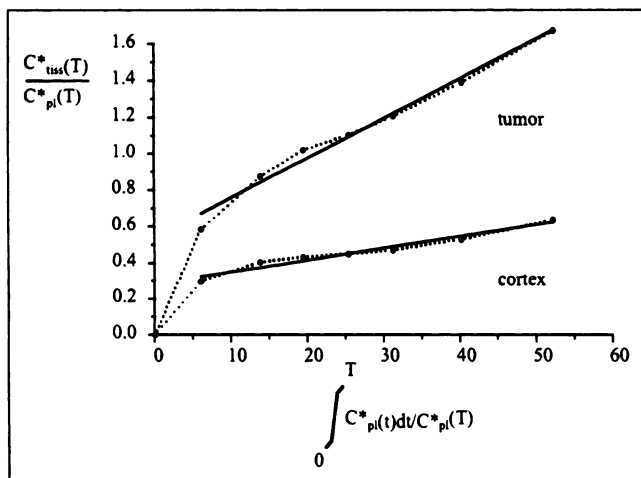


**FIGURE 8.** Gjedde-Patlak analysis of L-[<sup>18</sup>F]FET accumulation in a recurrent astrocytoma (tumor) and contralateral normal tissue (cortex).

Because a specific transport system is characterized not only by its saturability, but often by its stereoselectivity as well (32), the brain uptake kinetics of the enantiomer D-[<sup>18</sup>F]FET was also studied. Although we have no direct proof for a carrier-mediated transport of L-[<sup>18</sup>F]FET, the drastically smaller BBB permeability of D-[<sup>18</sup>F]FET compared with L-[<sup>18</sup>F]FET seems to indicate the transport by a carrier. The L-[<sup>18</sup>F]FET/D-[<sup>18</sup>F]FET uptake ratio is approximately 12 at 10 min postinjection and approximately 25 at 20 and 40 min postinjection. When compared with brain uptake data observed by Oldendorf (32), the stereospecificity of FET is significantly higher than that of phenylalanine or tyrosine and resembles that of dihydroxyphenylalanine (DOPA). These data are different from those observed with [<sup>11</sup>C]methionine, which show significant brain uptake for both isomers (33,34). Brain uptake of FET by diffusion through the BBB cannot be significant in view of its low lipophilicity. Recently, Heiss et al. (unpublished data) have shown by in vitro cell studies that the uptake of L-[<sup>18</sup>F]FET can be significantly inhibited with BCH (2-aminobicyclo-[2.2.1]-heptane-2-carboxylic acid) as a competitor for the L-amino acid transport system.

Like other artificial amino acids, L-[<sup>18</sup>F]FET accumulates in tumors. Our studies in mice bearing colon carcinoma SW 707 or mammary carcinoma MaCaF showed a high accumulation of L-[<sup>18</sup>F]FET in the tumor tissue. This again seems to indicate an increased influx constant  $K_i$ .

In the patient studied with L-[<sup>18</sup>F]FET and PET, the tracer showed a significant tumor accumulation with a tumor-to-cortex ratio of approximately 2 at 10 min after injection and approximately 2.7 at 40 min postinjection. It is surprising, but in accordance with the results in animal experiments, that L-[<sup>18</sup>F]FET is trapped in both tumor and normal brain tissue. Gjedde-Patlak analysis of the data up to 40 min (Fig. 8) showed linearity for the tumor and reference brain tissue, indicating trapping at least during the observation period

(tumor:  $K_i = 1.76$  mL/min/100 g,  $r = 0.99$ ; cortex:  $K_i = 0.74$  mL/min/100 g,  $r = 0.91$ ).

The whole-body scan showed no significant activity accumulation in peripheral organs at 40 min postinjection. In contrast to the animal experiments, no significant activity concentration was observed in the pancreas. The reason for this species difference is unclear.

## CONCLUSION

L-[<sup>18</sup>F]FET is a promising <sup>18</sup>F-labeled amino acid for imaging cerebral and, possibly, peripheral tumors. High in vivo stability, fast brain and tumor uptake kinetics, stereoselective brain uptake, low accumulation in nontumor tissue and ease of synthesis strongly support further evaluation of L-[<sup>18</sup>F]FET as an amino acid tumor tracer. The high imaging contrast obtained with L-[<sup>18</sup>F]FET is also ideal for coincidence scanners.

Further experiments are needed to clarify the mechanisms of transport and retention in the brain. In contrast to [<sup>11</sup>C]methionine, L-[<sup>18</sup>F]FET did not accumulate in bone marrow, kidney or pancreas and, thus, may have potential application in the detection of peripheral tumors. L-[<sup>18</sup>F]FET may find widespread application, because it can be produced in large yields.

## ACKNOWLEDGMENTS

This work was supported in part by the Deutsche Krebshilfe Grant 10-0972-Se 1. We thank the crew of the RDS 112 cyclotron for <sup>18</sup>F production, the PET team for excellent technical assistance and Ngoc Nguyen for editorial help.

## REFERENCES

- PET studies on amino acid metabolism and protein synthesis. In: Mazoyer BM, Heiss WD, Comar D, eds *Developments in Nuclear Medicine*. Dordrecht, The Netherlands: Kluwer Academic Publishers; 1993.
- Vaalburg W, Coenen HH, Crouzel C, et al. Amino acids for the measurement of protein synthesis in vivo by PET. *Nucl Med Biol*. 1992;19:227-237.
- Keen RE, Barrio JR, Huang SC, Hawkins RA, Phelps ME. In vivo cerebral protein synthesis rates with leucyl-transfer RNA used as a precursor pool: determination of biochemical parameters to structure tracer kinetic models for positron emission tomography. *J Cereb Blood Flow Metab*. 1989;9:429-445.
- Wiesel FA, Blomquist G, Halldin C, et al. The transport of tyrosine into the human brain as determined with L-[1-<sup>11</sup>C]tyrosine and PET. *J Nucl Med*. 1991;32:2041-2049.
- Comar D, Carton JC, Maziere M, Maranzo C. Labeling and metabolism of methionine-methyl-<sup>11</sup>C. *Eur J Nucl Med*. 1976;1:11-14.
- Bolster JM, Vaalburg W, Elsinga PH, Wynberg H, Woldring MG. The preparation of DL-[1-<sup>11</sup>C]methionine. *Appl Radiat Isot*. 1986;37:1069-1070.
- Arnstein HRV, Richmond MH. Utilization of p-fluorophenylalanine for protein synthesis by the phenylalanine-incorporation system from rabbit reticulocytes. *Biochem J*. 1984;1:340-346.
- Bodsch W, Coenen HH, Stöcklin G, Takahashi K, Hossmann KA. Biochemical and autoradiographic study of cerebral protein synthesis with [<sup>18</sup>F]- and [<sup>14</sup>C]-fluorophenylalanine. *J Neurochem*. 1988;50:979-983.
- Coenen HH, Stöcklin G. Evaluation of radiohalogenated amino acid analogues as potential tracers for PET and SPECT studies of protein synthesis. *Radioisot Klin Forsch*. 1988;18:402-440.
- Coenen HH, Franken K, Kling P, Stöcklin G. Direct electrophilic radiofluorination of phenylalanine, tyrosine and DOPA. *Appl Radiat Isot*. 1988;39:1243-1250.
- Coenen HH, Kling P, Stöcklin G. Cerebral metabolism of 2-[<sup>18</sup>F]fluorotyrosine: a new PET tracer of protein synthesis. *J Nucl Med*. 1989;30:1367-1372.

12. Lemaire C, Guillaume M, Christiaens L, Palmer AJ, Cantineau R. A new route for the synthesis of [<sup>18</sup>F]fluoroaromatic substituted amino acids: no carrier added L-*p*-[<sup>18</sup>F]fluorophenylalanine. *Appl Radiat Isot*. 1987;38:1033–1038.
13. Inoue T, Tomiyoshi K, Higuichi T, et al. Biodistribution studies on L-3-[fluorine-18]fluoro- $\alpha$ -methyl tyrosine: a potential tumor-detecting agent. *J Nucl Med*. 1998; 9:663–667.
14. Wienhard K, Herholz K, Coenen HH, et al. Increased amino acid transport into brain tumors measured by PET of 2-[<sup>18</sup>F]fluorotyrosine. *J Nucl Med*. 1991; 32:1338–1346.
15. Ishiwata K, Kubota K, Murakami M, et al. Re-evaluation of amino acid PET studies: can the protein synthesis rates in brain and tumor tissues be measured *in vivo*. *J Nucl Med*. 1993; 34:1936–1943.
16. Heiss WD, Wienhard K, Wagner R, et al. F-Dopa as an amino acid tracer to detect brain tumors. *J Nucl Med*. 1996;37:1180–1182.
17. Ogawa T, Miura S, Murakami M, et al. Quantitative evaluation of neutral amino acid transport in cerebral gliomas using positron emission tomography and fluorine-18 fluorophenylalanine. *Eur J Nucl Med*. 1996;23:889–895.
18. Ito H, Hatazawa J, Murakami M, et al. Aging effect on neural amino acid transport at the blood-brain barrier measured with L-[2-<sup>18</sup>F]fluorophenylalanine and PET. *J Nucl Med*. 1995;36:1232–1237.
19. Biersack HJ, Coenen HH, Stöcklin G, et al. Imaging of brain tumors with L-3-[<sup>123</sup>I]iodo- $\alpha$ -methyl-tyrosine and SPECT. *J Nucl Med*. 1989; 30:110–112.
20. Langen KJ, Coenen HH, Roosen N, et al. SPECT studies of brain tumors with L-3-[<sup>123</sup>I]iodo- $\alpha$ -methyl-tyrosine: comparison with PET, <sup>124</sup>I-IMT and first clinical results. *J Nucl Med*. 1990;31:281–286.
21. Tislijar U, Kloster G, Ritzl F, Stöcklin G. Accumulation of radioiodinated L- $\alpha$ -methyl tyrosine in pancreas of mice: concise communication. *J Nucl Med*. 1979;20:973–976.
22. Kloster G, Bockslaff H. L-3-[<sup>123</sup>I]- $\alpha$ -methyltyrosine for melanoma detection: a comparative evaluation. *Int J Nucl Med Biol*. 1982;9:259–269.
23. Langen KH, Roosen N, Coenen HH, et al. Brain and brain tumor uptake of L-3-[<sup>123</sup>I]iodo- $\alpha$ -methyl tyrosine: competition with natural L-amino acids. *J Nucl Med*. 1991; 2:1225–1228.
24. Oldendorf WH. Brain uptake of radiolabeled amino acids, amines, and hexoses after arterial injection. *Am J Physiol*. 1973;221:1629–1639.
25. Wester HJ. N.c.a. *F-18-Fluorination of Proteins, Peptides and Tyrosin*. Report no. 3209. Juelich, Germany: Nuclear Research Center Juelich; 1996.
26. Block D, Coenen HH, Stöcklin G. N.c.a. [<sup>18</sup>F]fluoroalkylation via nucleophilic fluorination of disubstituted alkanes and application to the preparation of *N*-[<sup>18</sup>F]fluoroethylpiperone. *J Lab Compds Radiopharm*. 1986;23:1042–1044.
27. Block D, Coenen HH, Stöcklin G. N.c.a. [<sup>18</sup>F]fluoroalkylation of H-acidic compounds. *J Lab Compds Radiopharm*. 1986;25:185–200.
28. Hawkins RA, Huang SC, Barrio JR, et al. Estimation of local cerebral protein synthesis rates with L-[<sup>11</sup>C]leucine and PET: methods, models, and results in animals and humans. *J Cereb Blood Flow Metab*. 1989;9:446–460.
29. Schober O, Meyer GJ, Duden C. Amino acid uptake in brain tumors using positron emission tomography as an indicator for evaluating metabolic activity and malignancy. *Rofo Fortschr Geb Rontgenstr Nuklearmed*. 1987;147:503–509.
30. Wester HJ, Dittmar C, Herz M, Hamacher K, Schwaiger M, Stöcklin G. Synthesis and biological evaluation of O-2-[F-18]fluoroethyl)-L-tyrosine ([F-18]FET) ([<sup>18</sup>F]FET) [abstract]. *Nuklear-medicin*. 1997;36:A75.
31. Wester HJ, Dittmar C, Herz M., Senekowitsch-Schmidtke R, Schwaiger M, Stöcklin G. Synthesis and biological evaluation of O-(2-[<sup>18</sup>F]fluoroethyl)-L-tyrosine (FET): a potential PET tracer for amino acid transport [abstract]. *J Nucl Med*. 1997;38:175P.
32. Oldendorf WH. Stereospecificity of blood brain barrier permeability to amino acids. *Am J Physiol*. 1973;224:967–969.
33. Schober O, Meyer G, Hundeshagen H. Brain tumor imaging using C-11-labeled L-methionine and D-methionine. *J Nucl Med*. 1985;26:98–99.
34. Bergström M, Lundquist H, Ericson K, et al. Comparison of the accumulation kinetics of L-(methyl-<sup>11</sup>C)-methionine and D-(methyl-<sup>11</sup>C)-methionine in brain tumors studied with positron emission tomography. *Acta Radiol*. 1987;28:225–229.